

DESIGN OF FIBER-REINFORCED CELLULAR STRUCTURES WITH TENSEGRITY BEHAVIOR MANUFACTURED USING 3D PRINTED SAND MOLDS

Nikhil Jorapur^{1,2}, Robert West², Christopher B. Williams^{1,2}, Alan Druschitz³

¹ Design, Research and Education for Additive Manufacturing Systems Lab

³ Virginia Tech Foundry Institute for Research and Education

² Department of Mechanical Engineering

³ Department of Material Science & Engineering

Virginia Tech, Blacksburg, VA 24060

Abstract

Tensegrity structures provide a high stiffness to mass ratio since all the comprising elements are either in compression or tension. However, they have limited applications since fabrication of such structures is challenging due to their complexity and mainly requires manual assembly of components. The authors look to Additive Manufacturing (AM) as a means to introduce tensegrity behavior in cellular structures to enhance structural performance. Specifically, octet cellular structures are created by casting aluminum into 3D-printed sand molds embedded with continuous wires. In this paper, the authors describe design and analysis of octet cellular structures that feature high strength fibers held in continuous tension. Finite element analysis of 4-point bending test is used to evaluate the effectiveness of embedded fibers. Also, the presence of tensegrity behavior was evaluated using this analysis and testing. The structure with tensegrity behavior was found to be 30 % stronger. The simulation and experimental results were shown to match within 6 % error in the elastic region.

1 Introduction

1.1 Cellular Materials

Cellular materials are a set of lightweight structures, which provide sufficient stiffness and strength with a lower mass density for a particular loading [1] [2]. These structures are of great interest due to their efficient structural performance and have been developed for a wide range of applications in automotive, bio-medical, aerospace, sporting, construction and energy-absorption systems [3]. Cellular structures are characterized by a network of cells comprising inter-connected struts, which help in reducing material present in the structure [2]. They are differentiated by the nature of the voids present in the structure. Stochastic materials are composed of cells of random shape, morphology and distribution [4]. Ordered/periodic cellular materials are composed of an ordered repetition of standard cell topology [5]. Cellular materials featuring designed mesostructures are differentiated by their selective placement of material to achieve multiple design objectives (i.e., the topology is repeatable and controlled but not necessarily periodically repeating) [5].

Recent efforts have been directed to improve performances of cellular structures. Using stiffer, higher strength materials, compressive stiffness and strength can be increased. Through fabrication of lattices at millimeter scale it is shown that the cellular structure can withstand higher axial stresses [6], [7], [8]. This is simply because materials gain strength at lower scales, which implies high elastic modulus in structures can make them significantly stronger.

Additive Manufacturing (AM) has enabled progress in improving processes, design and materials for fabricating cellular materials with designed mesostructures. Electron beam melting (EBM) process was used to manufacture Ti-6Al-4V auxetic structures with negative Poisson's ratio, which were shown to be superior compared to regular foam structures [9]. Projection microstereolithography was used to produce octet microlattices exhibiting ultrastiff properties without being affected by density [10]. In this paper, the authors aim to increase the bending stiffness of octet-cellular structures through incorporation of tensegrity behavior realized by reinforcement of continuous high strength fibers. In this context, AM is used to solve the manufacturing challenges to realize tensegrity behavior.

Fiber-reinforced cellular composite structures have been proposed as a means of solving structural limitations of cellular materials and bridging the space between current materials and unachievable low-density region in Ashby's chart [11]. Micro-buckling failure in struts of pyramidal truss structures was improved through carbon-fiber reinforced polymer laminates [12]. Unidirectional carbon fiber/epoxy prepreg laps were hot-pressed to form pyramidal structures with superior compressive strength. [13]. Sandwiched composite foldcores with carbon-reinforcement were produced to enhance the brittleness of the structures enabling better energy-absorption [14]. Hollow composite trusses composed of carbon-fibers were arranged to form pyramidal truss structures with high buckling strength using thermal expansion molding [15]. Composite cellular materials were processed by reversibly assembling and integrating looped fiber composite beams in a millimeter scale, which extended stretch-dominated lattice structures to ultra-light regime [16]. Silicon-carbide filaments were reinforced inside the titanium struts to fabricate millimeter scale lattice structures outperforming other cellular materials with density of less than 1 g cm^{-3} [17], [18].

1.2 Context: Tensegrity Structures

Tensegrity arrangement is designed to involve only tensile and compression stresses regardless of loading style [19]. The word tensegrity is a reduction of *tensile integrity*, coined by R. B. Fuller through his patent in 1962 [20]. The structure is made of spatial assemblies of rigid compressive bars and deformable pre-stressed strings [21]. Their non-linear mechanical behavior along with minimal mass formations [22] for given loads make them suitable for lightweight deployable applications. Tensegrity structures can also absorb and distribute energy under different load conditions [23], [24]. The strings help in distribution of compressive stress of rods through their pre-tension and high strength. A robotic leg was created using the tensegrity arrangement of bone-tendon such that pre-tensioned wires were included to absorb energy and enable high speed running [25]. However, their applications are limited due to the manufacturing challenges caused by complexity and are often fabricated by manual assembly. In order to address this gap, the authors present the use of a process chain of Additive Manufacturing (AM) and metal-casting.

The effort towards fiber-reinforcement of cellular materials can be approached through a tensegrity perspective. In this paper, authors aim to embed continuous long fibers such that tensegrity behavior is introduced in cellular structure, consequently improving the structural performance. The study reported in this paper concentrates on developing performance of octet cellular structures for bending applications.

1.3 Context: Octet Cell Structure

Most of the instances where bending loads are subjects, cellular structures are significantly used [6], [7], [26], [27]. Cellular structures with stretch dominated cores have been produced to predominantly experience axial stresses when loaded in bending [6], [18]. Also, their performance is considered to be superior to panels, whose struts deform by bending. Octet unit cell, as shown in Figure 1 is considered to be stretch dominated core where predominantly axial stresses are experienced under bending loads [1]. These cores which experience axial stress in bending can be complemented by fiber, which can act as pre-stressed strings to introduce tensegrity behavior, making the structures more efficient. Also, it would be nearly pure tensegrity behavior, since there would be little presence of bending stress in such core structures [6].

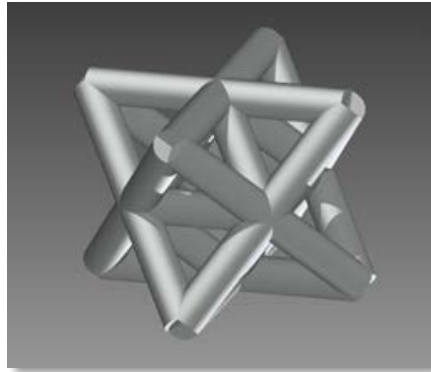


Figure 1. Octet 3D cell structure

In this paper the authors present the method of introducing the tensegrity behavior in octet cellular structures through finite element analysis. The authors describe the design of structure and fabrication process made possible through AM and traditional casting techniques. Section 3 describes the concept of locating fibers such that they are loaded in tension. Section 4 discusses the modeling of octet cellular structure with fibers following methods from Section 2. The tensegrity behavior is also studied in this section. Section 4 describes the fabrication methods and experimental testing on the structures. Results are discussed in last section with a closure of the work reported in this paper.

2 Background and Motivation

2.1 Limitations of Cellular Materials

While cellular materials provide superior structural performance, their applications are constrained by lower elastic moduli and indentation weakness [2] [28]. These structures are predominantly affected by concentrated compressive stresses [29]. Also, the core of the panel suffers local yield or crushing accompanied with face sheet stretching/tearing [30], [31], [32]. All these limitations are reported to be affected by strength of the core and cell size [33].

2.2 Continuous Fiber-Reinforcement

Nature provides best examples in exhibiting mechanical efficiency where often continuous long fibers are observed to enhance structural performance. Investigation on pomelo fruit, which can withstand a drop of 10 m without significant damage, has revealed that the peel consists of

hierarchical cellular structures with fibrous supports that boost energy absorption, as shown in Figure 2 [34]. In an effort to create a man-made structure with similar properties, the same research group attempted to produce metal-metal composite structure to mimic pomelo's behavior. Aluminum with two different variants of ductility, outside shell being less ductile was constructed and evaluated for energy absorption [35].

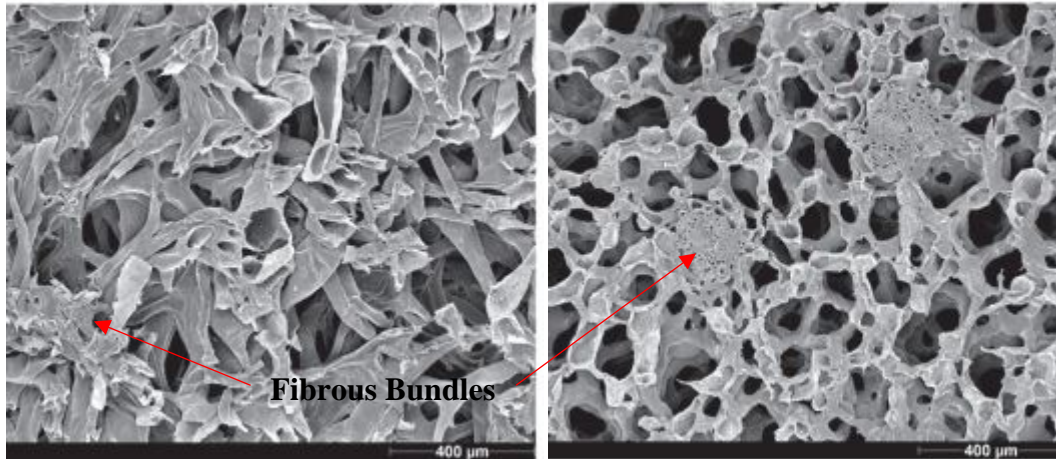


Figure 2. SEM images of pomelo peel samples [34]

In this paper, the work has been inspired by the presence of continuous fibers in the aforementioned structures, where performance in terms of energy-absorption and strength has been enhanced. Using these continuous fibers authors seek to introduce tensegrity behavior and provide another answer to improve cellular structures. For this solving manufacturing challenges imposed by tensegrity structures is important. Actuated joints were created by embedding shape memory alloys using Polyjet 3D printing process [36]. Copper wire was embedded in fused deposition modeling process using ultrasonic energy [37]. Figure 3 represents the basic approach followed in this paper. For embedding fiber in any AM system, the print needs to be paused to embed fiber and continue printing to attain the final part.

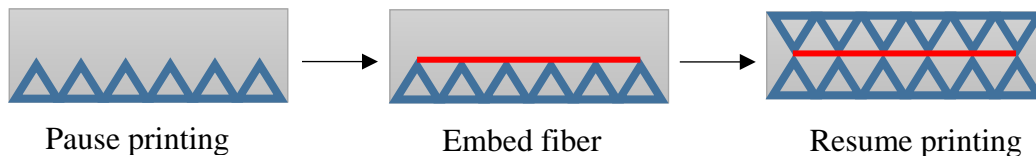


Figure 3. Schematic representation of embedding fiber while 3D printing

3 Modeling and Analysis

The purpose of modeling was to make design decisions such as truss dimensions, placement of fiber and validating tensegrity behavior in cellular structures. Finite element analysis on two-dimensional truss arrangements and octet 3D beams structure was conducted in ABAQUS/Explicit [38] to produce a design of cellular structures with tensegrity behavior.

In order to integrate tensegrity behavior it is important to determine the placement of fiber, such that the load distribution occurs due to the tensioning of fibers. This study was expanded and applied to octet-cellular structure. The presented analysis technique can be effectively used to include tensegrity behavior in other cellular materials.

For the analysis studies, Aluminum 6061-T6 was chosen as the material for trusses and cellular structures. The material was assumed to isotropic, homogeneous and hookean for elastic deformations. The material was given an elastic modulus of 68.9 GPa [39] and Poisson's ratio of 0.33 [39]. The structures are subjected to 4-point bending test since the structure is being designed for a bending application. Bending performance is evaluated in terms of stresses and displacements occurring in the elastic region.

3.1 Concept

A two-dimensional arrangement of trusses was created to provide basis of the concept. Figure 5 (a) depicts the structure, which was studied to establish the concept of including high-strength fibers to achieve tensegrity mechanics in cellular structures. This study was an inexpensive method to represent cellular structures and provide guidance while embedding fibers.

3.1.1 Truss Dimensions

Using the curve Euler-Johnson curve for aluminum as reference, the truss dimensions were chosen such that the struts did not fail due to buckling. Strut diameter was chosen to be 7 mm to ensure the complete filling of mold while casting and also allow enough bonding with fiber. It is essential for bonding to occur so that the wires are engaged completely in tension. The wires would otherwise slip in their place and not contribute towards reduction of stress concentration. For a slenderness ratio of 24.5, the strut length was chosen to be 25 mm.

3.2 Truss 2D Finite Element Modeling

The structure, as shown in Figure 5 (a), was subjected to 4-point bending test where the loads were applied parametrically and the displacement of the center point was noted for each loading condition. The truss-structure were all represented by 2D beam elements – B21, the Timoshenko beam elements meant for short columns. The loading and boundary conditions were set for 4-point bending tests. The loading points are indicated Figure 4. One end of the structure was pinned while the other end was allowed to move only in X-direction (roller) as shown in Figure 5 (a).

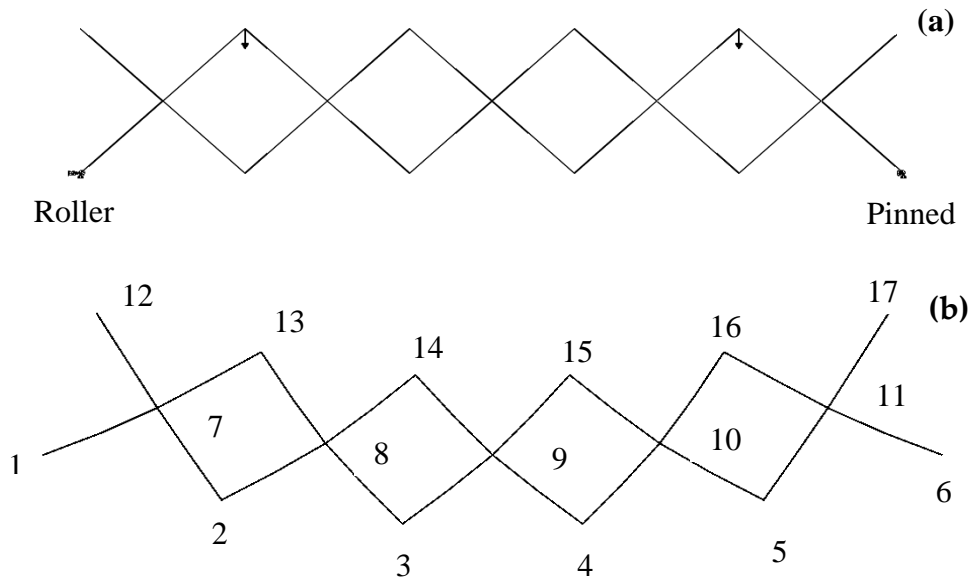


Figure 4. 2D Truss a) loading and boundary conditions, b) deformed state after loading

3.2.1 Results

The displacement of the points in the 2D Truss structure was studied. Nodes 1, 2, 3, 7, 8 and 9, as shown in **Figure 5**, were considered since the structure is symmetric and the displacements would be the same for the corresponding mirrored nodes. Also the nodes on the top will have the negative displacement with the same magnitude as the corresponding bottom nodes.

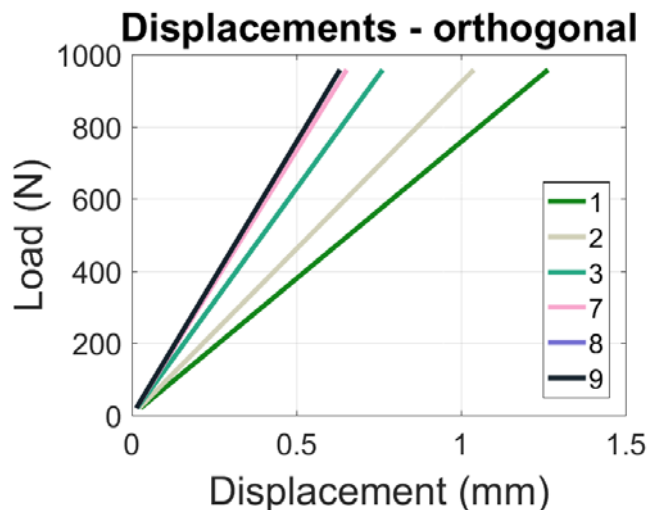


Figure 5. Displacements (orthogonal to loading direction) at selected nodes

Points where displacement occurred orthogonally to the loading direction were noted. Nodes 1, 2 and 3 show high displacements, which means nodes its true for nodes 4, 5 and 6 as well. These points are candidates for continuous fiber reinforcement. If a fiber were to be placed at these points, the displacements along the orthogonal direction would cause the fiber to be placed in tension, and thereby distributing the stresses from struts. Displacements are nearly zero at the

point lying in center since they lie on the neutral axis if this truss arrangement is considered as beam.

2D-analysis of the same truss-arrangement with fiber inclusions was conducted to test the effect of fiber. One basic assumption is that the bonding between the truss and fiber is considered to be perfect. The material properties of the truss, meshing scheme, loading and boundary conditions all remained the same as the previous study. For the fiber material stainless steel wire type 302 (elastic modulus = 193 GPa [40]) was chosen with a standard 1/8 inch diameter. The fiber was modeled as a T2D2 (no bending) truss element with no-compression to deactivate, as fibers do not provide stiffness against compression loading. Figure 6 (a) shows the placement of fibers.

The fibers were placed on the top layer to maintain the symmetry of structure for loading. The truss arrangement is considered to be a section of a larger structure and hence the fibers were located in the center as well to show that they would engage otherwise. It is important to note that the fibers connect the nodes of the cellular structure to fulfill the purpose of incorporating tensegrity behavior. Also, due to the pre-stressing, the fibers in the top layer would engage even if they are under compression. However, this paper does not concentrate on the effects of pre-stress but rather lays out the concept of fiber-arrangement such that tensegrity behavior is seen.

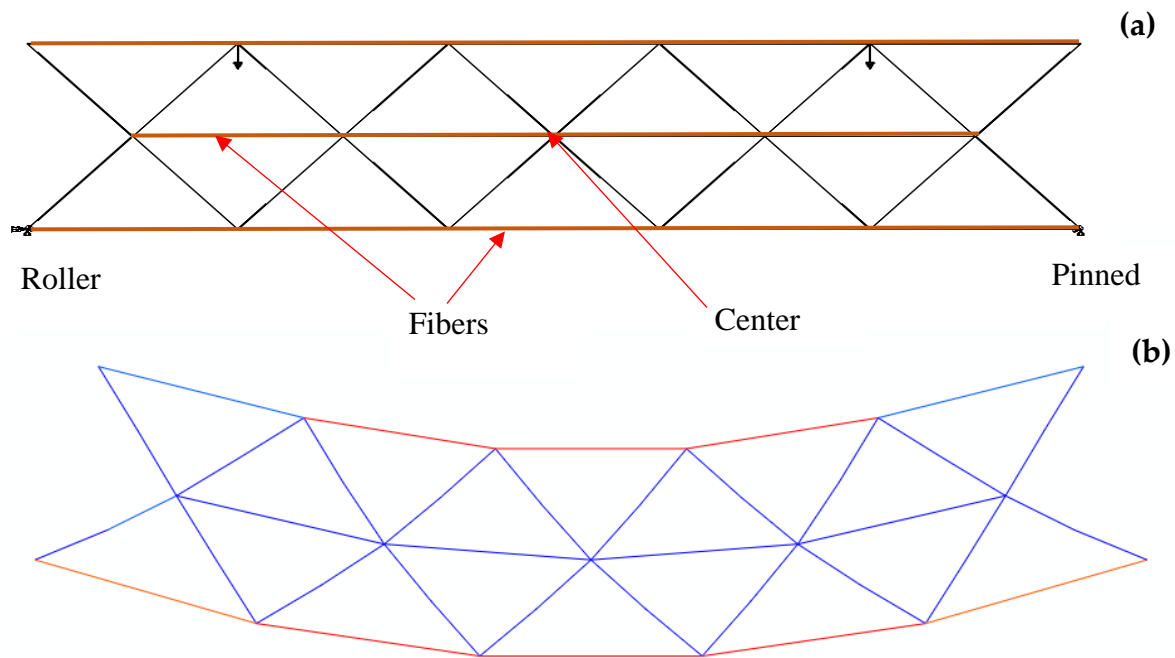


Figure 6. a) Fiber - included in truss, b) Deformed truss with fibers

Figure 6 (b) represents the deformation of structure with fibers. The performance was measured in terms of displacement in direction of loading at the center of the structure and the stresses associated with it. Figures 7 (a) and (b) depict the displacement (Y-direction) and stress of the center and for parametric loading on the structures respectively. The slope of curve for truss with fiber is greater, implying the structure has become stiffer.

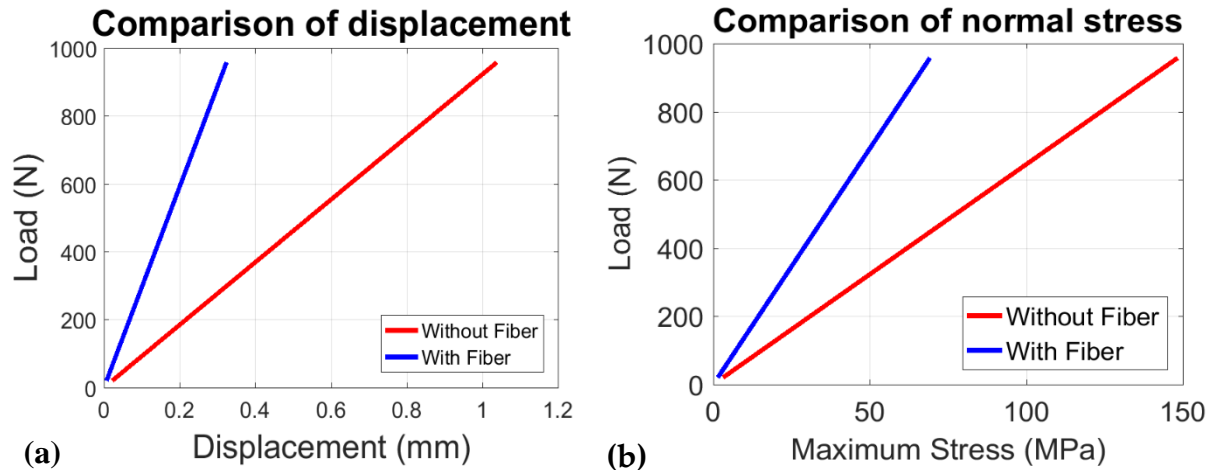


Figure 7. (a) Load vs displacement at center, (b) Load vs stress at center

It can be noted that the slope of the curve with fiber is much steeper. Stresses in truss with fibers decreased by 79 MPa. This improvement in strength can be attributed to the appropriate location of fibers, which have been engaged in tension to reduce stress. The displacement was decreased by 0.43 mm by fibers making the structures stiffer. The effectiveness of fibers included in structures was convincing to place them in octet cellular structures using the same methodology.

3.3 Octet- Cellular Structure Modeling

As proved in 2D truss-analysis the fiber inclusions do make the structures stronger and stiffer. 3D Beam analysis was conducted on octet structures to understand the physics of structures and gain insight into the placement of fibers.

A 3D Beam structure was built to represent octet geometry as shown in **Fig. 8 (a)**. The strut dimensions were based on the same slenderness ratio as selected in Section 3.1. Nine octet cells were repeated in length and two in width to form a structure suitable for 4-point bending test. The overall dimensions were 318.20 mm x 70.71 mm x 35.35 mm. The structure was assigned Al-6061 T6 material with B-31 mesh elements. This was specifically done to confirm the magnitude of bending stress present in the structure. The loading and boundary conditions for 4-point bending test were assigned as shown in **Fig. 11 (a)**.

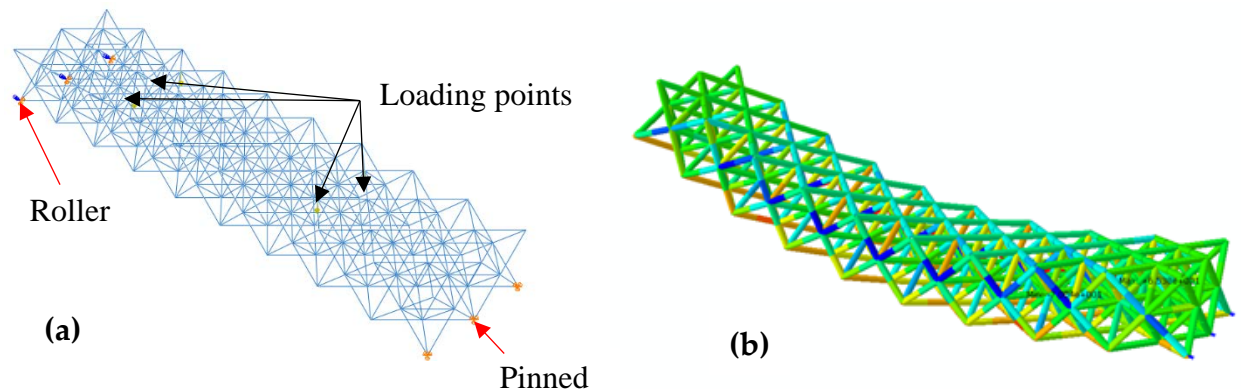


Figure 8. (a) Octet cellular with loading and boundary conditions, (b) Deformed octet structure

The deformation of the structure was studied as shown in Fig. 15 (c). Fibers were included at points as chosen in Section 3.2. The fiber material remained the same as mentioned in Section 3.2.1. As depicted in Fig. 9 (a), 3D-beams octet structure was modeled with fibers. As in the 2D model (Section 3.2), the fibers were represented as T3D2 no-compression truss elements since they have no stiffness against compression loads and cannot experience bending loads. Similar loading and boundary conditions were provided as that shown in Fig. 9 (b).

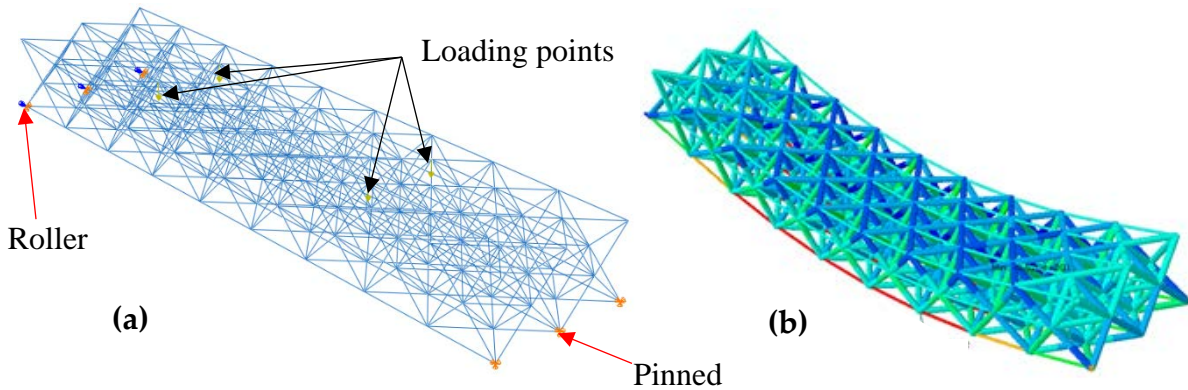


Figure 9. (a) Octet structure with fibers-loading and boundary conditions, (b) Deformed structure

3.3.1 Results

Figure 9 (b) shows the deformations occurring in octet structure with steel wires. The deformations in both the octet structures were studied in terms of stresses and displacements. Figure 10 (a) and (b) represent the displacement at the loading points and maximum stress observed in structures for parametric loading respectively.

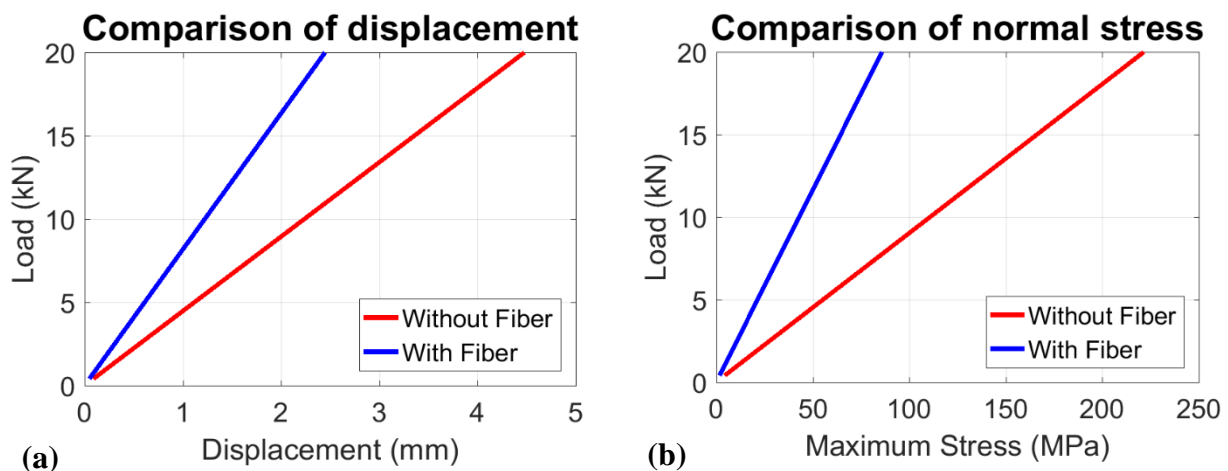


Figure 10. (a) Load vs displacement at center, (b) Load vs stress at center

Table 1 provides the details of effectiveness of steel wires through displacements and normal stresses due to the presence of steel wires. The stiffness of the structure with steel wire

increased through reduction in vertical displacement by 2 mm. Increase in strength due steel wires was about 178.3 MPa, which underlines the effect of tensegrity behavior.

Table 1. Effectiveness of fibers

	Maximum Displacement (mm)	Maximum Stress (MPa)
Octet Structure	4.4	253.4
Octet Structure with steel wires	2.4	75.1

3.4 Tensegrity Observation

The bending stress in both the structures was studied as shown in Fig. 11 (a). The tension experienced in all bottom wires were studied, as shown in Fig. 11 (b).

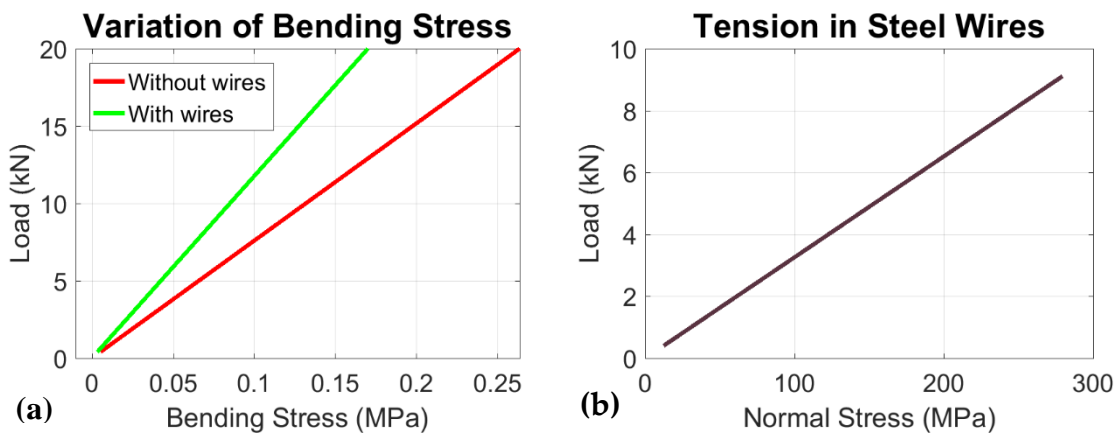


Figure 11. (a) Bending stress in octet structure with wires (b) Tension in steel wires

There is reduction of these stresses in octet structure with wires. This is attributed to the interplay between octet cellular shape and the tension in steel wires. This interplay is a consequence of tensegrity behavior where the tension in wires can effectively engage to reduce the stress due to the shape of the cell and wire arrangement.

As observed in there is presence of bending stress in octet structure with wires, but the value is very low. The structure does not experience much of bending stress due to the octet arrangement. The tension in steel is seen to be increasing with the load. The structure with wires is shown to be stiffer and stronger through results in Table 1. This behavior is typical of tensegrity structures. Due to the presence of some small bending stress it is stated to be nearly tensegrity behavior.

4 Experimental Test and Validation

4.1 Fabrication

A manufacturing process to produce complex cellular metal composites using Binder Jetting AM process was established [41]. The process makes use of sand molds printed through Binder Jetting technology and metal is directly cast into them to produce the final part. In this paper the aforementioned process was adapted to produce cellular structures with fiber-reinforcements as shown in Fig. 12.

The mold arrangement was split such that fiber embedding could be achieved. The mold-designs were created through a Boolean subtraction of Octet design from a block of exact overall dimensions. Molds were printed using the CAD-designs using Binder Jetting AM technology. The wires were embedded in the molds and the mold-setup was complete with additional packing of sand around it to secure the positions of wires. For this mold, A356 alloy was poured, which is a common aluminum alloy (Al-7wt%Si-0.3wt%Mg) [42] with a good combination of mechanical properties and castability. The temperature of metal in furnace was limited to 754.44 °C (1390 °F). The temperature while pouring, although not measured, is expected to be ~10-20 °C lower than the furnace. As shown in Fig. 12, the structure was successfully embedded with steel wires to attain a final part resembling the structure in Fig. 9. Another structure without wires was fabricated alongside to complete the comparison study while testing.

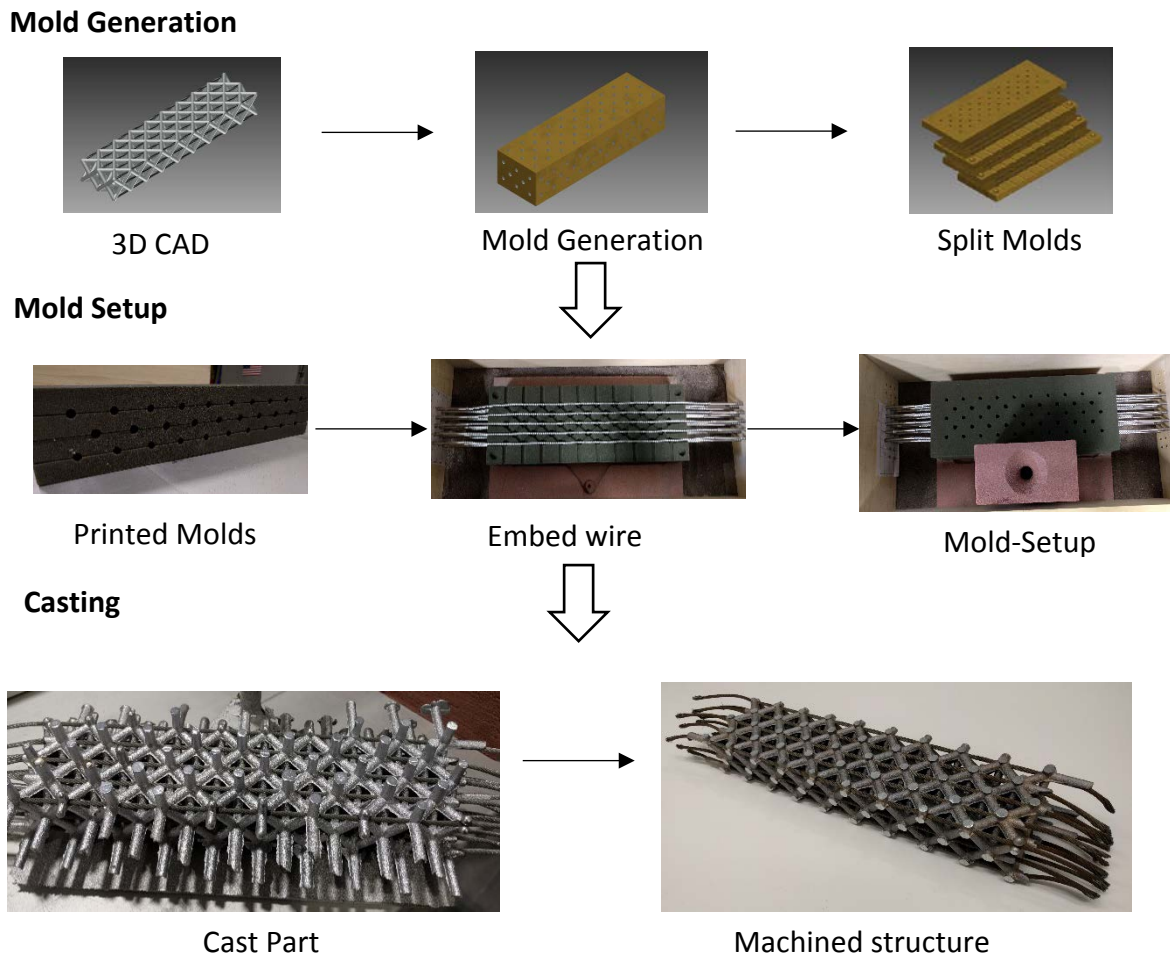


Figure 12. Process to create cellular structures with tensegrity behavior

The weights of both structures were measured after machining with fiber-reinforced octet structure at 1.44 kg while the one without wires was 1.16 kg.

4.2 Testing

Four-point bending test was carried out on both the fabricated structures using a testing fixture built for this. The test was conducted on MTS Insight using the control module provided

by MTS. Figure 13 (a) shows the structures set on the fixtures for testing. The region between loading points were subjected to constant bending moment and zero shear force. The maximum value of bending moment is to be found in this region. Tests were conducted at constant displacement rate of 2 mm/min to achieve quasi-static loading condition according to the military standards: MIL-STD-401 DIN 53291.

The displacement of loading points and the loading data were acquired during the tests. Figure 13 (b) indicates the maximum displacements caused in both the structures during the test for the acquired loads.

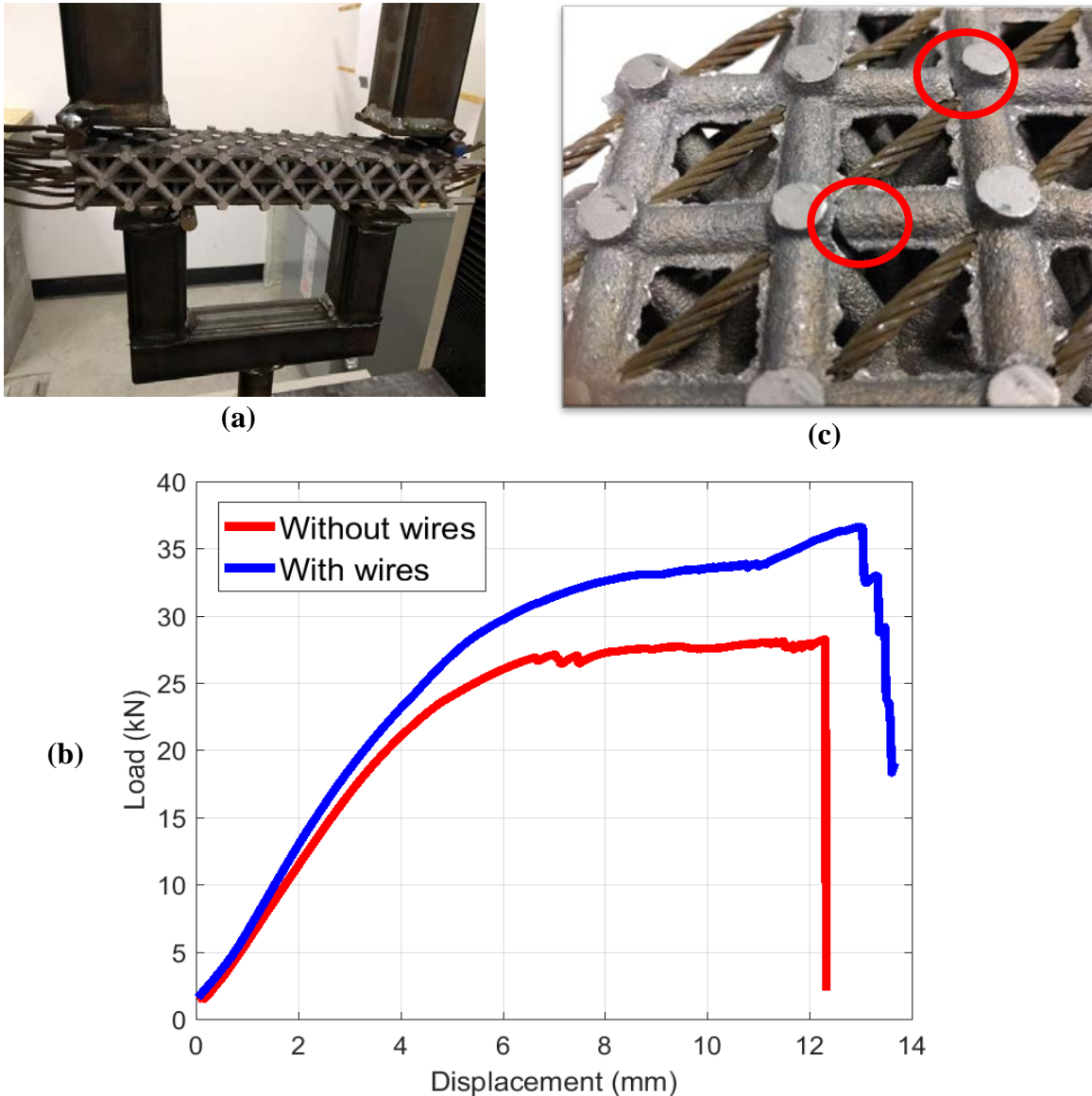


Figure 13. (a) Four point bending test setup (b) Comparison of load and deflection in octet structures with and without steel wires

The load needed to cause failure in octet structure with steel wires is observed to be 36.59 kN, which is 8.348 kN more than the failure load for octet structure without wires. The slope of

the curves (difference in slope - 1100) in elastic region as shown in Fig. 13 (b) suggest that the bending stiffness of octet structure with steel wires is larger, proving the structure for better performance.

As shown in Fig. 13 (c) the failure first occurs in aluminum strut and the steel wires are still intact. The steel wires are still engaged and this increases the ultimate strength of the structure. The wires are seen to perform more efficiently in the plastic region since they were not pre-stressed initially but only held in enough tension to engage while testing. In the plastic region the wires are at their maximum potential and hence the ultimate strength is observed to have increased more than the stiffness.

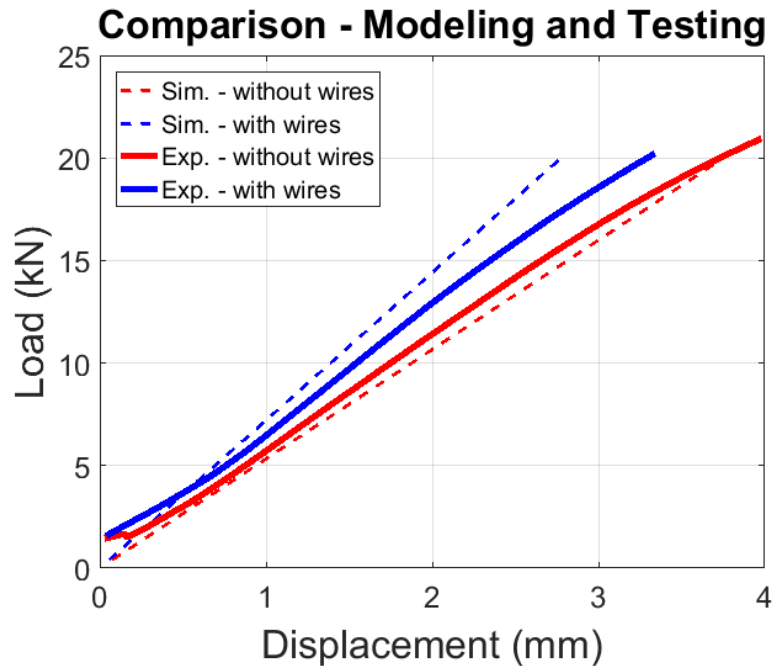


Figure 14. Comparison – Simulation and Experiment

Figure 14 depicts the differences between the simulation and experimental testing in the elastic region. For octet structure with wires the discrepancy is less than 3 %. This error can be due to the non-uniformity of struts in the fabricated parts. While the struts were designed to be of diameter 7 mm, this wasn't achieved. The average strut diameter was found to be around 7.3 mm, which makes the structure stiffer than the simulation. At lower strains, for the structure with wires the error is around 6 % while at higher strains it is around 15 %. This discrepancy can be attributed to the bonding issues between the wires and aluminum. The simulation perfect bonding while in reality this may not be achieved.

5 Closure and Future Work

2-D finite element analysis of 4-point bending test was conducted on a truss-arrangement to understand the mechanics and establish a method for the placement of fibers. The bending stresses experienced by octet structures, while wires engaged in tension to reduce stresses

indicating nearly tensegrity behavior was achieved. 3-D beam analysis of octet structures with fibers showed improvements in strength and stiffness due to incorporation of tensegrity behavior.

The fibers effectively reduced the stress from adjacent sections by engaging in tension. The structures without wires experienced normal stress of about 253.4 MPa while the structures with wires reported stress of about 75.1 MPa. In the analysis it was seen that octet structures with fibers experienced very little bending stress (about 0.25 MPa). Nearly tensegrity behavior was achieved to improve strength and stiffness during 4-point bending test as discussed in Section 3.4. The octet structures were successfully fabricated through process chain as indicated in Fig. 12. Fiber-embedding was successfully accomplished in fabrication through molds created by using Binder Jetting AM technology.

For an increase in weight of 0.28 kg, the octet structures with steel wires demonstrated higher stiffness and strength by failing at 36.59 kN. The same increase in strength can be achieved with even less weight-increase if fibers such as carbon-fiber, silicon-carbide and alumina are used since their stiffness to mass ratio is considerably higher than steel wire.

In the future, a 3D solid model will be constructed for finite element analysis and validate experiments by simulating the 4 point bending test. The effects of fiber would be studied thoroughly to establish a criteria of design. A study on pre-stressing would help in increasing the overall stiffness of the structure and ultimate strength to a greater extent than what is observed in this study. Material characterization will be carried out to understand the bonding between steel wire and aluminum.

6 Acknowledgements

This material is based upon work supported by the National Science Foundation under Grant No. 1462089. Any opinions, findings, and conclusions or recommendations expressed in this material are those of the author(s) and do not necessarily reflect the views of the National Science Foundation. The authors wish to thank Ex-One for 3D printing molds. Also, the authors thank Erin Connelly and Patrick O'Brien for their help during fabrication and testing.

References

- [1] V. S. Deshpande, N. A. Fleck, and M. F. Ashby, "Effective properties of the octet-truss lattice material," *Journal of the Mechanics and Physics of Solids*, vol. 49, pp. 1747–1769, 2001.
- [2] M. F. Gibson, J. W., Ashby, *Cellular Solids: Structures and Properties*. Cambridge University Press, Cambridge, UK, 1997.
- [3] J. Banhart, "Manufacture, characterisation and application of cellular metals and metal foams," *Prog. Mater. Sci.*, vol. 46, no. 6, pp. 559–632, Jan. 2001.
- [4] D. W. Nguyen, J., Park, S. I. and Rosen, "Cellular structure design for lightweight components," in *Innovative Developments in Virtual and Physical Prototyping*:

- Proceedings of the 5th International Conference on Advanced Research in Virtual and Rapid Prototyping, p. p. 203.
- [5] C. B. Williams, F. Mistree, and D. W. Rosen, "Investigation of solid freeform fabrication processes for the manufacture of parts with designed mesostructure," vol. 84832, no. 404, pp. 1–13, 2005.
 - [6] V. Deshpande and N. Fleck, "Collapse of truss core sandwich beams in 3-point bending," *Int. J. Solids Struct.*, vol. 38, no. 36–37, pp. 6275–6305, Sep. 2001.
 - [7] N. Wicks and J. W. Hutchinson, "Optimal truss plates," *Int. J. Solids Struct.*, vol. 38, no. 30–31, pp. 5165–5183, Jul. 2001.
 - [8] J. C. Wallach and L. J. Gibson, "Mechanical behavior of a three-dimensional truss material," *Int. J. Solids Struct.*, vol. 38, no. 40–41, pp. 7181–7196, Oct. 2001.
 - [9] L. Yang, O. Harrysson, H. West, and D. Cormier, "Compressive properties of Ti–6Al–4V auxetic mesh structures made by electron beam melting," *Acta Mater.*, vol. 60, no. 8, pp. 3370–3379, May 2012.
 - [10] H. Lee, T. H. Weisgraber, J. Deotte, E. B. Duoss, J. D. Kuntz, M. M. Biener, Q. Ge, J. A. Jackson, S. O. Kucheyev, N. X. Fang, C. M. S. Ultralight, and C. Link, "Ultralight , ultrastiff mechanical metamaterials Accessed," 2016.
 - [11] M. F. Ashby and Y. J. M. Bréchet, "Designing hybrid materials," *Acta Mater.*, vol. 51, no. 19, pp. 5801–5821, Nov. 2003.
 - [12] K. Finnegan, G. Kooistra, H. N. G. Wadley, and V. S. Deshpande, "The compressive response of carbon fiber composite pyramidal truss sandwich cores," *Int. J. Mater. Res.*, vol. 98, no. 12, pp. 1264–1272, 2007.
 - [13] J. Xiong, L. Ma, L. Wu, B. Wang, and A. Vaziri, "Fabrication and crushing behavior of low density carbon fiber composite pyramidal truss structures," *Compos. Struct.*, vol. 92, no. 11, pp. 2695–2702, Oct. 2010.
 - [14] S. Heimbs, J. Cichosz, M. Klaus, S. Kilchert, and a. F. Johnson, "Sandwich structures with textile-reinforced composite foldcores under impact loads," *Compos. Struct.*, vol. 92, no. 6, pp. 1485–1497, May 2010.
 - [15] S. Yin, L. Wu, L. Ma, and S. Nutt, "Pyramidal lattice sandwich structures with hollow composite trusses," *Compos. Struct.*, vol. 93, no. 12, pp. 3104–3111, Nov. 2011.
 - [16] K. C. Cheung and N. Gershenfeld, "Reversibly Assembled Cellular Composite Materials," *Science (80-.)*, vol. 341, no. 6151, pp. 1219–1221, Sep. 2013.

- [17] P. Moongkhamklang, D. M. Elzey, and H. N. G. Wadley, "Titanium matrix composite lattice structures," *Compos. Part A Appl. Sci. Manuf.*, vol. 39, no. 2, pp. 176–187, Feb. 2008.
- [18] P. Moongkhamklang, V. S. Deshpande, and H. N. G. Wadley, "The compressive and shear response of titanium matrix composite lattice structures," *Acta Mater.*, vol. 58, no. 8, pp. 2822–2835, May 2010.
- [19] Hanaor, "Geometrically rigid double-layer tensegrity grids," *Int. J. Sp. Struct.*, vol. 9, no. 4, p. 227, 1994.
- [20] R. B. Fuller, "Tensile-Integrity Structures," United States Pat. 3,063,0521.
- [21] F. Fraternali, L. Senatore, and C. Daraio, "Solitary waves on tensegrity lattices," *J. Mech. Phys. Solids*, vol. 60, no. 6, pp. 1137–1144, Jun. 2012.
- [22] R. E. Skelton, "Optimal tensegrity structures in bending: The discrete Michell truss," *J. Franklin Inst.*, vol. 347, no. 1, pp. 257–283, 2AD.
- [23] J. T. Scruggs and R. E. Skelton, "Regenerative Tensegrity Structures for Energy Harvesting Applications," *Proc. 45th IEEE Conf. Decis. Control*, pp. 2282–2287, 2006.
- [24] G. Tibert, "Deployable Tensegrity Structures for Space Applications," Doctoral Thesis, 2002.
- [25] A. Ananthanarayanan, M. Azadi, and S. Kim, "Towards a bio-inspired leg design for high-speed running.," *Bioinspir. Biomim.*, vol. 7, no. 4, p. 046005, Dec. 2012.
- [26] H. J. Rathbun, F. W. Zok, and a. G. Evans, "Strength optimization of metallic sandwich panels subject to bending," *Int. J. Solids Struct.*, vol. 42, no. 26, pp. 6643–6661, Dec. 2005.
- [27] N. Wicks and J. W. Hutchinson, "Performance of sandwich plates with truss cores," *Mech. Mater.*, vol. 36, no. 8, pp. 739–751, Aug. 2004.
- [28] M. F. Ashby, A. Evans, N. a Fleck, L. J. Gibson, J. W. Hutchinson, and H. N. . Wadley, "Metal foams: a design guide," *Mater. Des.*, vol. 23, no. 1, p. 119, Feb. 2002.
- [29] N. Harischandra, "System identification of muscle–joint interactions of the cat hind limb during locomotion," *Biol. Cybern.*, vol. 99, no. 2, pp. 125–138, 8AD.
- [30] D. E. Ingber, S. B. Bulletin, and N. Jun, "Cellular Basis of Mechanotransduction Stable," vol. 194, no. 3, pp. 323–327, 2016.
- [31] H. Wadley, "Fabrication and structural performance of periodic cellular metal sandwich structures," *Compos. Sci. Technol.*, vol. 63, no. 16, pp. 2331–2343, Dec. 2003.

- [32] S. Chiras, D. R. Mumm, a. G. Evans, N. Wicks, J. W. Hutchinson, K. Dharmasena, H. N. G. Wadley, and S. Fichter, "The structural performance of near-optimized truss core panels," *Int. J. Solids Struct.*, vol. 39, no. 15, pp. 4093–4115, Jul. 2002.
- [33] N. A. Fleck and V. S. Deshpande, "The Resistance of Clamped Sandwich Beams to Shock Loading," *J. Appl. Mech.*, vol. 71, no. 3, p. 386, 2004.
- [34] S. F. Fischer, M. Thielen, R. R. Loprang, R. Seidel, C. Fleck, T. Speck, and A. Bührig-Polaczek, "Pummelos as Concept Generators for Biomimetically Inspired Low Weight Structures with Excellent Damping Properties," *Adv. Eng. Mater.*, vol. 12, no. 12, pp. B658–B663, Dec. 2010.
- [35] S. F. Fischer, M. Thielen, P. Weiß, R. Seidel, T. Speck, A. Bührig-Polaczek, and M. Bünck, "Production and properties of a precision-cast bio-inspired composite," *J. Mater. Sci.*, vol. 49, no. 1, pp. 43–51, Nov. 2013.
- [36] N. A. Meisel, a. M. Elliott, and C. B. Williams, "A procedure for creating actuated joints via embedding shape memory alloys in PolyJet 3D printing," *J. Intell. Mater. Syst. Struct.*, Jul. 2014.
- [37] C. Kim, D. Espalin, A. Cuaron, M. a. Perez, M. Lee, E. MacDonald, and R. B. Wicker, "Cooperative Tool Path Planning for Wire Embedding on Additively Manufactured Curved Surfaces Using Robot Kinematics," *J. Mech. Robot.*, vol. 7, no. 2, p. 021003, Feb. 2015.
- [38] D. Systemes, "Abaqus Version 6.13." p. www.3ds.com, 2015.
- [39] "Aluminum 6061 T6 ; ASM Material Data Sheet," pp. 6–7, 2016.
- [40] "AISI Type 302 Stainless Steel , ASM Material Data Sheet," pp. 6–7, 2016.
- [41] D. Snelling, Q. Li, N. Meisel, C. B. Williams, R. C. Batra, and A. P. Druschitz, "Lightweight Metal Cellular Structures Fabricated via 3D Printing of Sand Cast Molds," *Adv. Eng. Mater.*, vol. 17, no. 7, pp. 923–932, Jul. 2015.
- [42] D. Snelling, C. Williams, A. Druschitz, and V. Tech, "A Comparison Of Binder Burnout And Mechanical Characteristics Of Printed And Chemically Bonded Sand Molds," pp. 197–209.